Conference Proceedings

Solar World Congress 2015
Daegu, Korea, 08 – 12 November 2015

Refractive based solar tracker with fixed concentration spot

Héctor Garcia[1], Carlos Ramirez[1] and Noel Leon[1]

[1] Tecnológico de Monterrey, Campus Monterrey, Monterrey (México)

Abstract

Solar energy has become one of the most promising renewable energies being the most widespread used nowadays. In order to achieve an optimum performance, both photovoltaic and solar thermal applications require the use of some kind of solar tracking technique. A solar tracking concentrator (STC) has to adapt to the changes in the sun's position throughout the day and even more so, throughout the year.

The present paper attempts to describe in detail the design of a state-of-the-art STC in which the concentration spot is fixed. The tracking system is based on refracting the sunlight onto a constant direction, contrary to existing solutions which reflects it. Having a constant direction of radiations makes possible to implement a stationary Fresnel lens to concentrate the solar power for any application desired. The system is designed and validated using mathematical models and simulation software to prove the feasibility of the concept.

Keywords: *Solar tracking system, solar concentration, solar energy, refraction*

1. Introduction

Most research efforts on solar energy have focused on photovoltaic (PV) cells development, however, commercial PV cells have only achieved an efficiency of 15% to 20% so far (Green et al. 2009), while high concentration photovoltaic (HCPV) have efficiency slightly above 40% (Pérez-Higueras et al. 2011).

Another research line explores the use of solar thermal energy (STE), in which case two main issues must be overcome. Firstly, solar radiation must be concentrated for high temperature applications; this is due the low density nature of such energy. Secondly, for most solar concentrators, solar rays must fall perpendicular to the concentrator at all times. Therefore, a solar tracking concentrator (STC) must be used. These requirements also apply for HCPV.

This work was carried on to explore the feasibility of a STC using a semi-passive solar tracking device consisting in two arrays of prisms and a Fresnel lens. A peculiarity of the system is the fixed position of the Fresnel lens therefore, if the prism array can indeed track effectively the sun's path there will be a constant position concentration spot that can be used either in HCPV or CSP applications.

Achieving this constant spot is non-trivial and could represent an important breakthrough since having a non-constant spot means that the receiver which captures the energy must move along with the tracker, elevating in many cases the cost of implementation.

2. Design of the STC

2.1 Concept Layout

The presented STC is an optic system that concentrates solar radiation with minimal movement. It has two layers of PMMA triangular prisms one placed above the other that redirect the received solar rays in a constant vertical direction toward a fixed Fresnel lens. Prism within a layer are identical one another. The first array of prisms rotate all of its components to the same angle, its rotation axis is parallel to the y-axis. In a similar manner, the second set of prisms rotate synchronously but having a rotation axis parallel to the x-axis. Both layers are located directly above a Fresnel lens as seen in Fig. 1.

doi:10.18086/swc.2015.04.09 Available at http://proceedings.ises.org

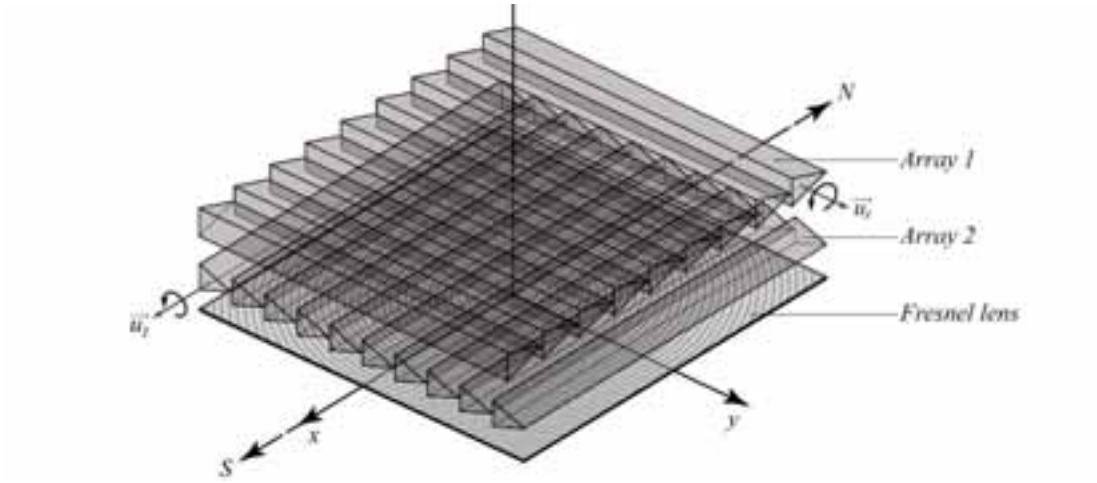

Fig. 1: STC system concept with fixed Fresnel lens

Figure 2 shows the lateral views of the proposed concept. This configuration allows to have the Fresnel lens in a fixed horizontal position; which significantly reduces the wind loads and more importantly it offers the virtue of having a stationary concentration spot, unlike many other STC which have a robust mechanical tracker that has to support all the moving components.

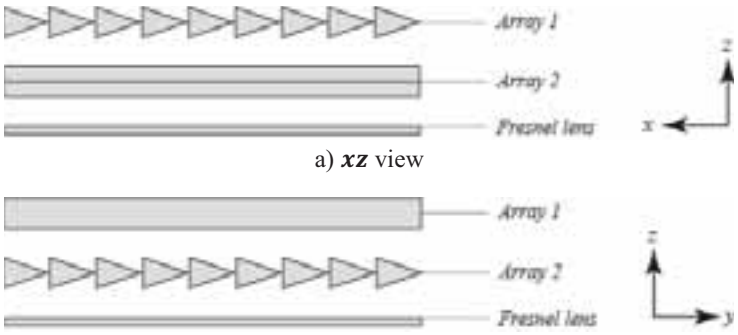

a) $\boldsymbol{xz}$ view

b) $\boldsymbol{yz}$ view

Fig. 2: STC system concept - XZ and YZ view

2.2 Prism

The initial concept employs triangular prisms, with the peculiarity that the polyhedron has an isosceles triangle as base, whose equal side's measure l and form an angle of ε. Prism's depth or height is h, as shown in Fig. 3. In any given prism the rotation axis goes through the body's center of mass, since prism are uniform longitudinally this coincides with the triangular gravicenter of the base. Consequently, the resultant torque due to gravity vanishes (Hibbeler, 2006).

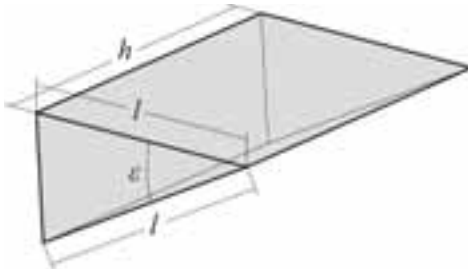

Fig. 3: Prism's dimensions

Since the rotation is the same within an array only one actuator for the mechanical movement is needed. The

mechanism can be idealize as a four-bar linkage similar to a window shutter but instead of blocking the sun's light, they redirect those solar rays by the refraction throughout the PMMA prisms.

There are two sets of prisms, upper and lower layer are identified by sub index 1 and 2 respectively. The prisms' inner angle are ε_1 and ε_2, as shown in Fig. 4. These values are not necessarily the same, although within each array all PMMA elements must be identical to one another.

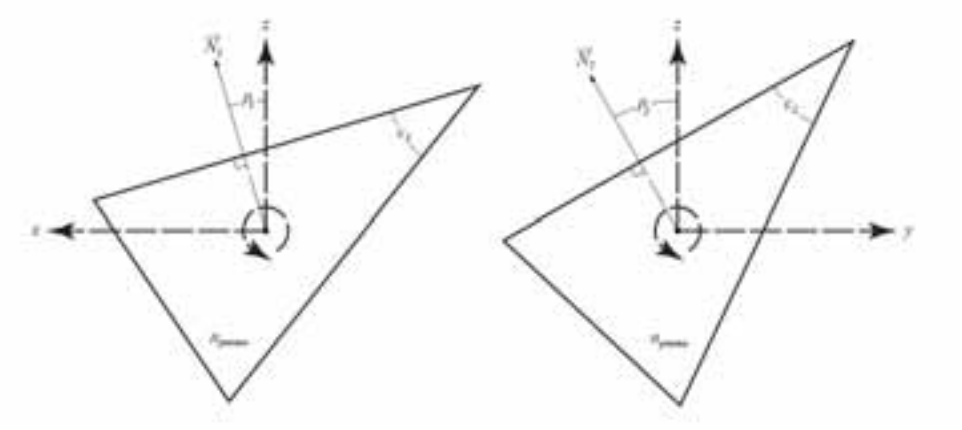

a) Upper layer b) Lower layer

Fig. 4: Prism's parameters

The geometry and refractive index are the key parameters of the prism. The design assumes that all prisms within the array are identical in both key parameters, thus the angle of rotation is shared, allowing the array to be driven by a single actuator. Additionally, this concept contemplates both upper and lower arrays to be made of the same material, however such consideration is not necessary.

Figure 4a shows the upper layer geometry, rotation axis is parallel to system's y-axis and a rotation by an angle of ρ_1; likewise Fig. 4b illustrates lower layer prism geometry with rotation axis parallel to system's x-axis and prism rotation by an angle ρ_2. For both cases the default position and reference point for the measurement of the rotation angle is referenced to the z-axis and the normal vector to the face of the prism.

2.3 Light Trajectory

Figure 5a illustrates required trajectory of the solar rays to successfully reach the receiver. For illustrative purpose only one prism of each layer is shown. The circular mark indicates where the beam changes medium. Emphasizing that the rays B and D are within the respective prisms. The upper layer is the first part of the system responsible for starting the solar tracking. Prisms rotate an adequate angle ρ_1 as shown in Fig. 5b to obtain the following trajectory:

A. Solar rays from the sun: These beams change direction throughout the day, they reach the 1st array of prisms and refract according to Snell's law.

B. Solar rays within the prisms of the 1st array: Inside the prism rays travel until reaching the opposite prism's side, where they exit by refracting when they change mediums.

C. Solar rays exiting the 1st array, toward 2nd array: These beams have the peculiarity of lacking a x component; this is accomplished by selecting ρ_1 accordingly. The path is presented in a XZ view, however exiting solar ray C not necessarily has a downward vertical direction, and has a non-zero y component as seen in Fig. 5c.

The following layer is located immediately below and it constitutes the second stage of the solar tracking system. Similarly prisms rotate an adequate angle ρ_2 as shown in Fig. 5c to obtain the following trajectory:

C. Solar rays from the 1st array: Coming from the upper layer, with the peculiarity of zero x component as described before. In other words ray is contained in plane YZ.

D. Solar rays within the prisms of the 2nd array: Inside the prism rays travel until reaching the opposite

prism's side, where they exit by refracting when they change mediums. Rays are also contained in plane YZ.

E. Solar rays exiting the 2nd array, toward Fresnel lens: These beams have the peculiarity of lacking both a x and y components; this is accomplished by selecting ρ_2 accordingly. Contrary to rays exiting from the first array, these beams do have a downward vertical direction.

The joint work of both arrays complete the tracking system, afterwards the solar rays must be concentrated into a fixed spot, and this is achieved by the next part of the system.

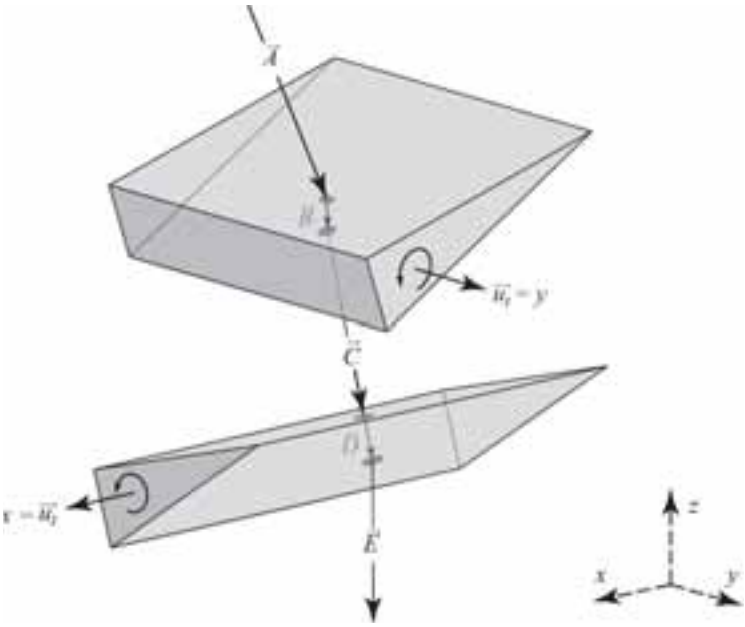

a) Isometric view

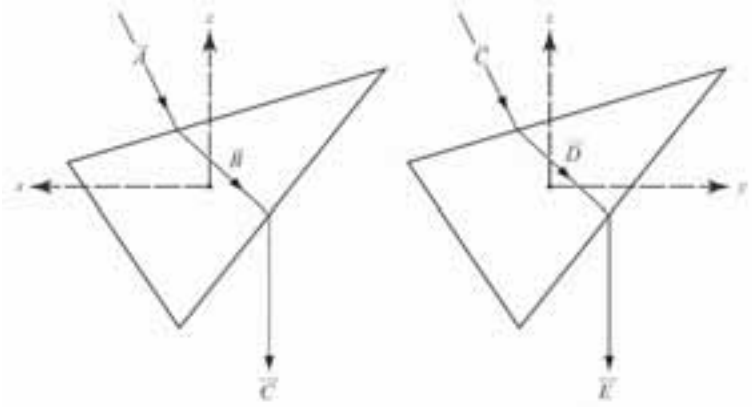

b) Upper layer: XZ view c) Lower layer: YZ view

Fig. 5: Ray's path through upper and lower layer.

2.4 Fresnel lens

The Fresnel lens is a type of compact lens that is able to concentrate solar energy in a reduced area; it is essentially a chain of prisms, in which each one represent the slope of a lens surface (Barone, 2005). The function of this optical device in the proposed system proposed is to receive the rays refracted by the two arrays of prisms and concentrate them in a fixed receiver. Since the solar rays reach the concentrator in a constant direction after going through both layers of prism, the lens can remain stationary.

3. Mathematical model

3.1 Dispersion by a prism

Many authors address the issue of the path of light through a prism, with one important consideration: it is assumed that the edge of the prism in which the two faces meet, with an angle ε, is perpendicular to the plane which contains the incident, transmitted, and emergent rays. (Born et al. 1999)

A ray entering a prism, as shown in Fig. 6, will emerge having been deflected from its original direction by an angle δ_{dev} known as the angular deviation. In terms of the SPSTC, this property is used to achieve the tracking as will be explain in detail later.

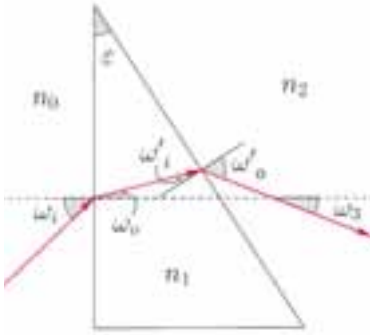

Fig. 6: Passage of a ray through a prism

Equations (1) and (2) are results of Snell's law, where n is the refractive index of the medium in question:

$$\omega_o = \sin^{-1}\left(\frac{n_0}{n_1}\sin\theta_0\right) \quad \text{(eq. 1)}$$

$$\omega'_o = \sin^{-1}\left(\frac{n_1}{n_2}\sin\omega'_i\right) \quad \text{(eq. 2)}$$

Additionally to Eqs. (3) and (4) are obtained by summation of angles, using the fact that the dashed line is perpendicular to the entrance face of the prism.

$$\omega'_i = \varepsilon - \omega_0 \quad \text{(eq. 3)}$$

$$\omega_3 = \omega'_0 - \varepsilon \quad \text{(eq. 4)}$$

For a prism in air as in the proposed concept, $n_0 = n_2 \simeq 1$. Defining $n_1 = n_{pmma}$, the deviation angle δ_{dev} is given by

$$\delta_{dev} = \omega_i + \omega_3 \quad \text{(eq. 5)}$$

Substituting Eqs. (1) to (4) into (5) yields:

$$\delta_{dev} = \omega_i + \sin^{-1}\left(n_{pmma}\sin\left[\varepsilon - \sin^{-1}\left(\frac{1}{n_{pmma}}\sin\omega_i\right)\right]\right) - \varepsilon \quad \text{(eq. 6)}$$

Abelman [2008] proposed a simplification of Eq. (6) if the incident angle ω_i and prism apex angle ε are both small, $\sin\theta \approx \theta$ and $\sin^{-1} x \approx x$, an important remark is that angles are expressed in radians. This allows the nonlinear equation in the deviation angle δ_{dev} to be approximated by:

$$\delta_{dev} \approx \omega_i + \left(n\left[\varepsilon - \left(\frac{1}{n}\omega_i\right)\right]\right) - \varepsilon \quad \text{(eq. 7)}$$

$$= \omega_i + n\,\varepsilon - \omega_i - \varepsilon \quad \text{(eq. 8)}$$

$$= (n - 1)\varepsilon \quad \text{(eq. 9)}$$

Furthermore the refractive index depends on wavelength λ, therefore for a thin prism the deviation angle varies with wavelength according to:

$$\delta_{dev}(\lambda) \approx [\,n(\lambda) - 1\,]\,\varepsilon \quad \text{(eq. 10)}$$

Considering to Eq. (6), it's evident that the deviation suffered by a monochromatic beam throughout a given prism is a function only of the incident angle at the first face, since apex angle ε and refractive index are fixed. Figure (7) shows a plot of the deviation angle for $n = 1.48$, for a variety of apex angles.

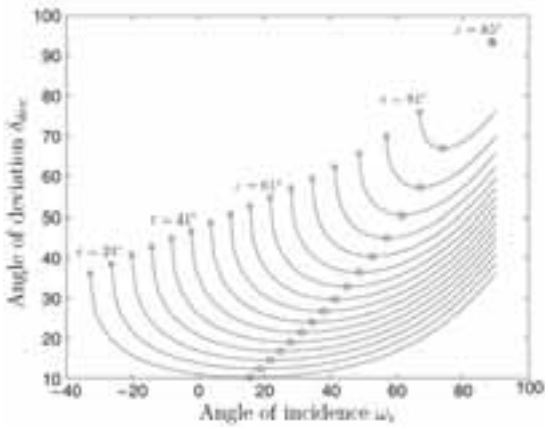

Fig. 7: Deviation δ_{dev} response to incident angle ω_i for several prism's apex angle ε (Abelman, 2008)

Figure 7 shows maximum and minimum deviation, for several values of ε, as squares and circles respectively. An important observation is how if the apex angle is increased the response plot tends to move up and to the right. Ultimately meaning a smaller range of admissible incident angles. For even larger apex angles, all rays that go inside the prism suffer a total internal reflection. On the contrary case if apex angle decreases too much, then Eq. (9) is a valid approximation and since refractive index is consider constant, then deviation depends solely on apex angle, which is also constant once implemented.

It should be notice that in the STC proposed the initial assumption described at the start of this section is not met for the first stage of the tracking system (upper layer). Since the plane which contains the incident, transmitted, and emergent rays is not always perpendicular to the prism edge; however, the repercussion apex angle has on deviation is a good starting point to understand how it affects the tracking system for redirecting sunlight. Furthermore another approach must be done to overcome the 3-dimensional ray.

3.2 Snell law in a 3-dimentional environment.

The physical phenomenon involved in this system, in both prisms arrays and Fresnel lens, is known as light refraction that obeys Snell's law. Nevertheless, the conventional form can only be applied when working in the same plane; however, the nature of solar rays' movement throughout the day and prism normal to the incident face produces non-constant working planes. Therefore, vector analysis must be performed to find an extrapolation of Snell's law for a 3-dimensional environment.

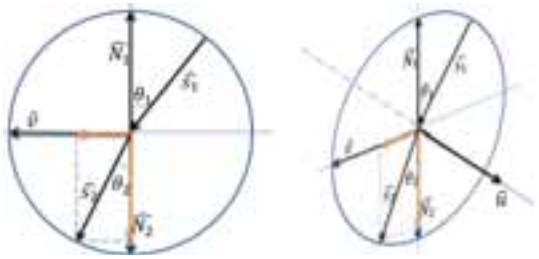

Fig.8: (a) Snell's law in a plane; (b) Snell's law in space

Equation (10) defines the output direction based on the orthogonal vectors that define the plane seen in Fig. 8a. An extrapolation of Snell's Law is shown in Eq. (11) in function of vectors $\hat{s}_1$ and $\widehat{N}_1$ only, which are the incident ray, and the normal vector to the surface, respectively. (Garcia et al, 2014)

$$\hat{s}_2 = (\sin\theta_2)\,\hat{v} + (\cos\theta_2)\widehat{N}_2 \qquad \text{(eq. 10)}$$

$$\hat{s}_2 = \frac{n_1}{n_2}\widehat{N} \times \left(-\widehat{N} \times \hat{s}_1\right) - \widehat{N}\sqrt{1 - \left(\frac{n_1}{n_2}\right)^2 \left(\widehat{N} \times \hat{s}_1\right) \cdot \left(\widehat{N} \times \hat{s}_1\right)} \qquad \text{(eq. 11)}$$

Equation (11) offers an analytical vectorial approach for light refraction; therefore, it is necessary to express incoming rays as unit vectors that represent the beam's direction, and the normal vector to the surface where rays incident.

3.3 Solar ray's directional vector

Figure 9 shows the direction of incoming solar rays. Setting the coordinate system as shown, where South and East coincide with x and y-axis respectively. Based Duffie and Beckman (1991) solar altitude α and azimuth γ may be obtained given a solar latitude, therefore the directional vector may be calculated.

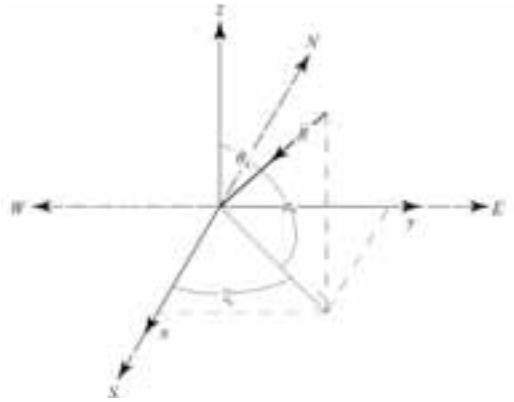

Fig. 9: solar ray in vector form

$$\vec{R}_{\gamma_s,\alpha_s} = -\cos(\alpha_s)\cos(\gamma_s)\,\hat{x} - \cos(\alpha_s)\sin(\gamma_s)\,\hat{y} - \sin(\alpha_s)\,\hat{z} \qquad \text{(eq. 12)}$$

Given any point of the year directional vector $\vec{R}_{\gamma_s,\alpha_s}$ is obtained. These beam will strike onto a prism, for which the normal vector to the plane must be calculated. This can be achieve rather easily doing a 2-dimensional analysis depending solely on the apex angle ε and the rotation ρ given to the prism

4. Solar Tracking

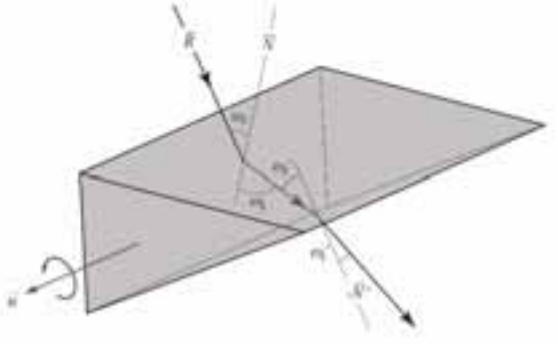

Fig. 10: Passage of a ray through a prism

Matlab implementation of mathematical model is based on Eqs. (11) and (12), functions are programed in order to know the path of light for any given parameters. One key element in the code is an analogy to the deviation formula, which for a given input ray's direction, incident normal vector is calculated and using Eq. (12) the direction inside the prism is obtained. Later internal normal vector in output face is computed to obtain the output direction of the path described by light beams as shown in Fig. 10

Tab. 1: Solar angles at given time at latitude $\varphi = 25°39'15''N$

Day of the year	120th
Solar time	10:30am
Solar azimuth angle (γ_s)	66.6257
Solar altitude angle (α_s)	66.2054

Tab. 2: Solar angles at given time at latitude $\varphi = 25°39'15''N$

Azimuth	Altitude	Incident solar ray		
γ_s	α_s	A_x	A_y	A_z
66.6257°	66.2054°	−0.160066	0.370348	−0.915

Given the solar angles, the directional components of solar rays are calculated, with the help of Matlab, the behavior of a ray through the prism for all possible rotations is obtained. The first stage of the STC is to control and eliminate if possible the component C_x, as stated earlier. It's important to realize that not all rotations generate an output ray, this happens when internally all light is reflected instead of being refracted, or if solar rays reach the prism at the non-active side of the triangle.

Figure 11a shows the behavior of x component for different apex angles ε_1 through all possible prism rotations ρ_1 (for a particular solar azimuth and altitude angles stated in Table 1).

It can be seen in Fig. 11 how if apex angle ε_1 increases the system will not be able to eliminate the desired component C_x; meanwhile when it does, there may be two rotations values: ρ_1 and ρ_1' that accomplish the desired output. Figure 11b shows a closer look to appreciate the points where response intersects horizontal line corresponding to $C_x = 0$.

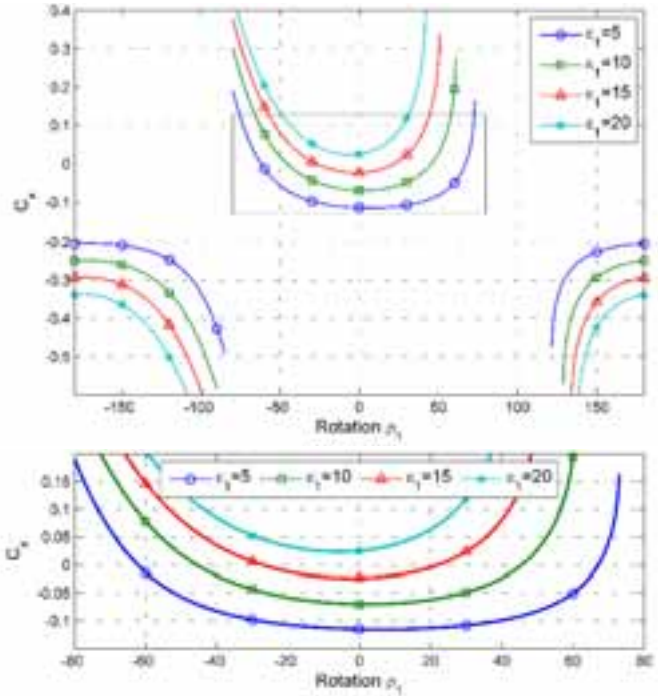

Fig. 11: a) Output response C_x for prism rotating ρ_1 for distinct values of ε_1, b) zoom view

Figure 12a shows the best rotation available for a wide range of apex angles that accomplish the minimum component $|C_x|$, meanwhile Fig. 12c shows component C_x achieve, for instance, in this particular case how apex angles higher than 17° can't achieve the desire output.

It can be proved that when rotation ρ_1 exist such that $C_x = 0$ then Eqs (13) to (15) stand true, meaning the output ray's direction is constant despite being multiple values of rotation ρ and independent to the prism apex angle ε.

$$C_x = 0 \qquad \text{(eq. 13)}$$

$$C_y = A_y \qquad \text{(eq. 14)}$$

$$C_z = \sqrt{1 - C_y^2} \qquad \text{(eq. 15)}$$

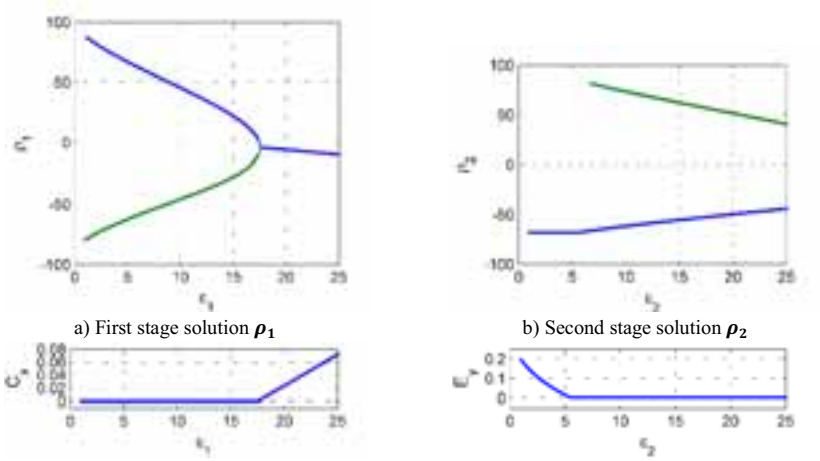

a) First stage solution $\boldsymbol{\rho_1}$ b) Second stage solution $\boldsymbol{\rho_2}$

c) First stage $\boldsymbol{C_x}$ output d) Second stage $\boldsymbol{E_y}$ output

Fig. 12: Best solution found for distinct values of apex angle $\boldsymbol{\varepsilon}$

Therefore despite the system's parameters for the 1st stage the rays will reach the 2nd stage in a given direction $\vec{C}$, from where the same analysis is perform to obtaining the best rotation available and the permissible apex angle to achieve the desire task.

5. Proof of concept

Additionally to the mathematical model a computer simulation using ray trace software and an idealized scale model consisting of two individual prism was constructed to corroborate the behavior of rays through the prisms. For instance the fact that given an input direction there exist different rotations that provide the same output can be seen in Fig. 13.

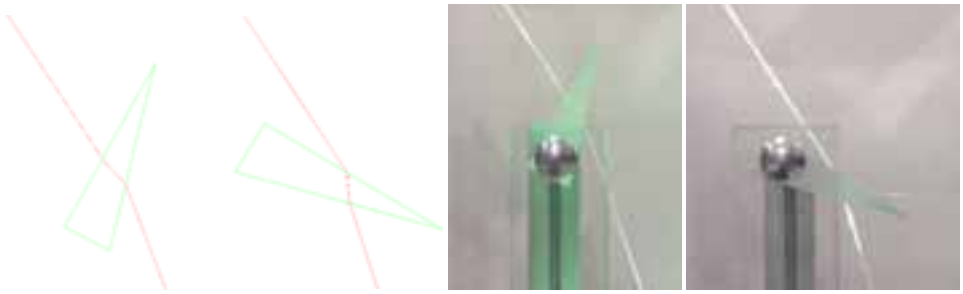

a) TracePro simulation b) Experimental model

Fig. 13: Two different rotation angles $\boldsymbol{\rho}$ with same output

An important remark is the Fresnel lens beneath the tracking system is not included in the model. Since initial design contemplates a conventional Fresnel lens to deal with the concentration part, the only requirement is that rays reach the lens perpendicularly to the surface.

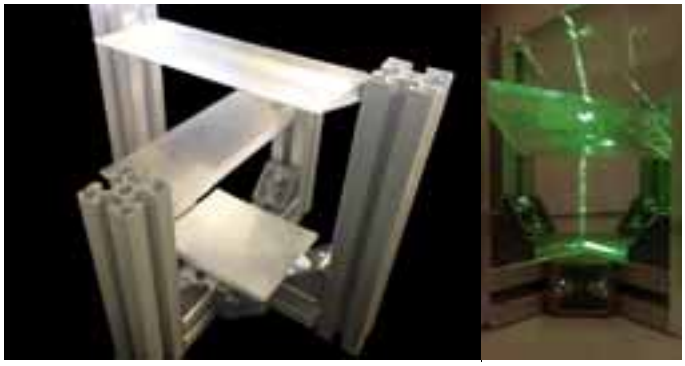

Fig. 14: Scale prototype as proof of concept

The present analysis was done for a particular time, however a deeper analysis is needed to see the system performance throughout the year, the fact that it works for an arbitrary moment does not assure the correct functionality for every day at all hours

6. System performance throughout the year

As stated before the behavior of solar angles throughout the year can be calculated as shown in Fig. 15, however we must acknowledge that the system may not be able to cover all possible solar values, therefore the system's target is set from 9 to 15hrs.

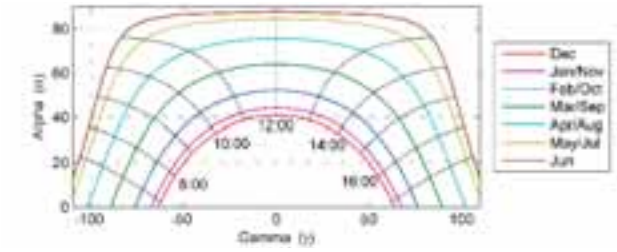

Fig. 15: Solar angles throughout the year, at latitude $\varphi = 25°39'15''N$

To view the tracker performance for a given pair of apex angles ε_1 and ε_2 the system is simulated via matlab to evaluate every possible pairwise values (γ, α) within the desired time window to apply the tracking algorithm and obtain the best output found. The primary interest is the angle θ formed between the theoretical direction $\vec{E}_s$ and the outcome ray $\vec{E}_r$ generated by the algorithm is closest to cero.

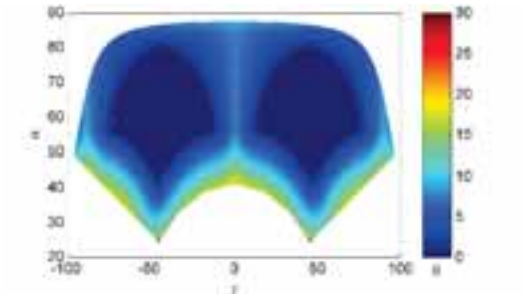

Fig. 16: Output ray variation θ from desire output with $\varepsilon_1 = 15.85$, $\varepsilon_2 = 15.28$

Notice there is a good tracking in two main areas shown in blue zones, however there is a gap at the center region $(\gamma = 0)$, additionally angles close to lower limit do not have a satisfactory response in the green zone.

6.1 Backtracking rays

Snell's refraction equation stands for both directions. Therefore one may think of refraction as a bijective function. Since the reversibility holds at each refracting surface, it holds also for even the most complicated light paths. In particular for the path define while going through an acrylic prism, as shown in Fig. 17a. Furthermore this same principle applies to the complete trajectory described by incoming solar rays and tracking system output rays as represented in Fig. 17b.

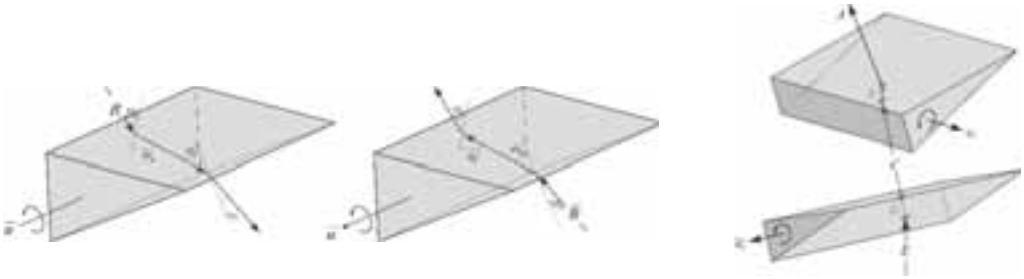

a) Throughout a single prism b) Through tracking system

Figure 17: Ray path in reverse direction

Therefore given a set of parameters ε_1 and ε_2 instead of doing the algorithm for every possible point (see fig. 15) a simpler approach arises which consists in calculating all possible reverse paths backtracking ray $\vec{E}$. This is simply obtained for every combination of rotation angles (ρ_1, ρ_2); graphing them to obtain a scatter plot that represents the system's admittance rays for which we can redirect accurately with $\theta = 0$, as shown in Fig 18.

Figure 18 shows just some simulations that were done, since plots are symmetrical only one side is computed. In the iterations the variations in ε shift the zone accordingly. Additionally the behavior of the system to ε also appears to have a direct correlation, as lower values tend to be close to upper limit and vice versa.

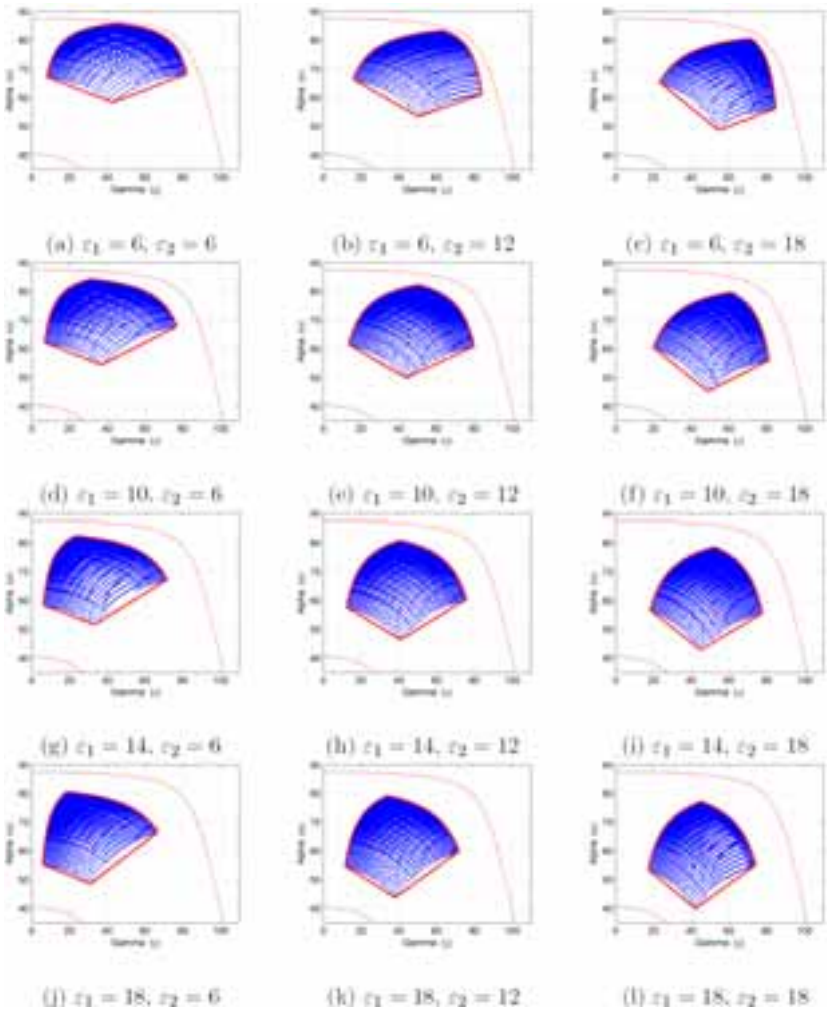

Fig. 19: Matlab simulation for different set of apex angles

7. Concluding remarks

A tracking algorithm was also implemented on Matlab to determine the required rotations values for a given time. The only design parameters for the present concept are the apex angles of the prisms in each layer, since the system relies on refraction of light there are physical constrains (Leutz and Susuki 2001): the critical angle plays an important role on the ability to correctly redirect light to the desire direction. For instance the second layer of prism al paths are in the same plane, since rays theoretically have $C_x = 0$, therefore analysis shown in Fig. 7 is valid, and deviation angle plays a direct role in the ability to redirect rays accordingly. Unfortunately this means that for times around noon $(\gamma = 0)$ the gap previously mention in Fig. 16 will always be present, since at that time the prism needs to give a null deviation, but from Eq. (9) that may only be achieve having a low apex angle sin refractive index is constant. From Fig. 7 we know that a low value of ε restrain of ability

to redirect rays, since the maxium deviation is restricted therefore a small apex angle helps the center gap but impairs zones where γ is close to the limit.

A STC is feasible using solely PMMA prism that rotate accordantly to the suns position, but with range of operation limitants. The selected values must be such that the time of operation of the system is maximized.

A three-dimensional mathematical model was developed to describe the path of a collimated light beam through a translucid solid medium. This vectorial approach was successfully implemented in Matlab being able to characterize the ray's path along the system, additionally a real life scale prototype and the TracePro computer simulation were used to validate the model.

The tracking is achieved by separating the dual axis movement and implementing two independent rotational movements that work hand by hand to refract efficiently solar rays. Doing so offers a simpler approach in tracking the Sun which ultimately would result in cheaper but reliable solution for most of the possible Sun's positions.

The current implementation has a fixed Fresnel lens which reduces greatly the mechanical effort of the system, since the tracking is performed by the rotating prisms arrays, which have the virtue of being lightweight individual prisms instead of a robust big heliostat, with the already mentioned trade-off.

A tracking mathematical algorithm was program in Matlab to obtain the best rotations for a given set of parameters $(\varepsilon_1, \varepsilon_2)$ throughout the year, however a deeper analysis must be done to understand the efficiency of the system.

The article presents a functional design and model capable of tracking the sun fairly well; nonetheless, there is still a vast area of opportunity for the improvement and optimization of the proposed STC. Additionally the presented work focuses on the light path toward a fixed objective, however light attenuation effects caused by the prism material must be furthermore studied to understand the real amount of energy the system can harvest from the sun.

8. Acknowledgement

The authors would like to thank the Institute of Renewable Energy (IER-UNAM) and the Mexican Center for Innovation in Solar Energy (CeMIE-Sol) for funding the present project through the Strategic Project #05: "Development of solar thermal storage units"; otherwise its development would have not been possible.

9. References

Abelman, S. and H. Abelman, Approximations of nonlinear phenomena arising in angular deviations of light rays that emerge from prisms. Computers & Mathematics with Applications, 55(3): p. 408-422. (2008)

Barone S, Directed Fresnel lenses. 2005, US Patent 2005/0041307A1.

Born, M., et al., Principles of Optics: Electromagnetic Theory of Propagation, Interference and Diffraction of Light, Cambridge University Press, 1999

Duffie J. and Beckman W.: Solar engineering of thermal processes. Wiley, 1991.

Garcia H, Leon N, Ramirez C, Rotating Prism Array for Solar Tracking. Energy Procedia. Volume 57, Pages 265–274, 2014

Green M., Emery K., Hishikawa Y., Warta W.: Progress in Photovoltaics: Research and Applications Solar. Cell Efficiency Tables. Volume 17, Issue 5, pages 320–326, 2009.

Hibbeler, R.C., Mecánica de materiales, Pearson Educación, 2006

Leutz R. and Suzuki A.: Non-imaging Fresnel Lenses: Design and Performance of Solar Concentrators. Springer, 2001.

Pérez-Higueras, P., E. Muñoz, et al.: High Concentrator PhotoVoltaics efficiencies: Present status and forecast. Renewable and Sustainable Energy Reviews 15: 1810-1815, 2011.